IJCSC 0973-7391 Vol 6 • Number 2 April - Sep 2015 pp. 159-174 **Impact Factor: 2.5** **Available at www.csjournals.com**

Validation of Fourier Mellin technique for Dermatoglyphic fingerprint pattern matching

[1] Mandeep Singh, [2] Oindri Majumdar
[1,2]Electrical and Instrumentation Engineering Department, Thapar University, Patiala, INDIA
[1] mandy_tiet@yahoo.com, [2] oindri_majumdar@yahoo.com

Abstract: Dermatoglyphics involves acquiring fingerprint images of all fingers of individuals and analyse their fingerprint patterns. It is scientifically proven that dermal ridge patterns are linked to our cerebral cortical makeup. Hence, correct pattern analysis can provide an insight to a person's inherent talents and potentials. However, while acquiring the images, lots of deformities alter the appearance. The images of same pattern maybe rotated by some minor angle or shifted from centre or even scaled, due to relative difference in sizes of fingertips of different individuals. For registering spatially transformed images of one pattern as same, Fourier Mellin transform is suggested and validated in this paper.
Keywords: Affine transforms, Dermatoglyphics, Fourier Mellin transform, Pattern matching.

1. INTRODUCTION

Dermatoglyphics [1] is the science of studying the ridged skin on a human body and analysing health, genetic diseases as well as cognition [2] and personality aspects of her. However, for doing so, one needs well enhanced and processed [3] fingerprint images of the subject. But, image acquisition is not always free from distortions. Image registration is a technique that aligns two similar images after they have undergone affine transforms. Affine transforms are either rotation by some angle, translation or shift in either horizontal or vertical direction. It may also include scaling of an image by some scaling factor. Although, the affine transforms happen inevitably, it is a must that an image be recognised as the original copy even after it has been torn and twisted. Hence, the Fourier Mellin transform is applied. It perfectly makes use of the characteristic features of both Fourier and Mellin transforms. Since the Fourier transform neglect time shift in frequency domain, the image translated in original plane gets fair autocorrelation in transformed domain. On the other hand, the Mellin transform performs normalized cross correlation to the affine transformed image and yet establishes high correlation, thus validating the originality of the image.Some fixed data points are decided upon the image in the coordinate plane. The affine transforms shall shift them from initial coordinates. The transformed data points are again observed at a different time, from a different angle or level or even from a separate sensor. The affine transformations once detected, can be used to set the test image in a manner so that it can be perfectly superimposed with the available template. When they are perfectly aligned, the algorithm finds a central pixel which is used a point of reference, against the correlation between the images.

2. METHODOLOGY

A. Affine Transformations

The affine transformation [4] are inevitable as far as acquisition of raw fingerprint images is concerned. While acquiring fingerprint images using electronic fingerprint scanners, it is very common for the images to vary in brightness, spatial resolution, clearness, etc. For accurate pattern recognition, the template needs to align to images of same pattern, taken at different times, under different conditions. Specially, where human fingerprints are concerned, human error like slight shift of finger press can cause a pattern to get smudged or rotated at some angle. It may also happen that due to varied size of digits of different subjects, same dermal ridge pattern might be scaled up for one subject than other. The methods generally consist of the following basic steps:

1. Detect features
2. Match corresponding features
3. Infer geometric transformations
4. Use the geometric transformation to align one image with the other.
5.

They might hamper the process of correct fingerprint pattern recognition due to the spatial ambiguity caused. A large number of false positive may arise. Hence, Fourier Mellin transform is applied. To check the accuracy of the method applied, correlationsbetween similar as well as different dermal patterns have been done. The results for correlation between similar dermal patterns have been shown in figure 1 to figure12. The different dermal patterns matched for the correlation, are displayed from figure 13to figure 45.

Any affine transformation is given by the transform which preserves the translation, rotation, shear, scaling, reflection, homothety etc. The affine transform is such that the transform perceives the input as original even

after there has been a rotation angle change in same plane, translation along horizontal and vertical direction. This is the reason why affine transforms are suitable for cylindrical coordinate system and not spherical coordinate system [5]. When there is any rotational change on an image, it occurs on same plane of cylindrical coordinate system. The spherical coordinate have two angular dimensions wherein images cannot be included. The z axis is taken as reference, as it is common to both Cartesian and cylindrical coordinate systems. Also, spherical coordinate cannot contribute to the understanding of translation given by $x_0$and y_0. Hence, cylindrical coordinates are the base for preserving collinearity of points in a straight line or proportionate ratio of distances and angles even after transformation. For example, if an image goes through scaling s, horizontal and vertical transformation of x_0 and y_0 and some rotation given by θ, then the rotation – enlargement algorithm is given by

$$\begin{bmatrix} x' \\ y' \end{bmatrix} = s \begin{bmatrix} \cos\alpha & \sin\alpha \\ -\sin\alpha & \cos\alpha \end{bmatrix} \begin{bmatrix} x - x_o \\ y - y_o \end{bmatrix}$$
$$= s \begin{bmatrix} \cos\alpha\,(x - x_o) + \sin\alpha\,(x - x_o) \\ -\sin\alpha\,(x - x_o) + \cos\alpha\,(x - x_0) \end{bmatrix}$$

If a = s cosα and b = s sinα
Then scale factor, s is given by

$$s \equiv \sqrt{a^2 + b^2}$$

And the rotation angle is given by

$$\alpha = \tan^{-1}\left(-\frac{b}{a}\right)$$

The Fourier – Mellin is an important tool for image registration. The resulting spectrum is invariant to rotation, scaling, translation etc.

B. Fourier Transform – Translation Invariant

The Fourier transform decomposes a function in time into its frequency components. It represents a complex value function which has a real and imaginary component. The real absolute value represents the magnitude of frequency at unit of original domain. The imaginary value gives the phase offset or the phase difference between two consecutive waves of same frequency. For an absolutely integral function f, of independent variable x representing time (in seconds) and transformed variable ξ representing frequency (in hertz)

$$\hat{f}(\xi) = \int_{-\infty}^{\infty} f(x) e^{-2\pi i x\xi}\, dt$$
$$= \int_{-\infty}^{\infty} g(u) e^{-2\pi i f(u+a)} du$$
$$= e^{-2\pi i f(a)} \int_{-\infty}^{\infty} g(u) e^{-2\pi i f(u)} du$$
$$= e^{-2\pi i f(a)}\, G(f)$$

The transform associates frequency domain representation to a function of time. The property of translation invariance can be understood from shifting property. If a function in time is shifted by some units, g(t-a), the resultant Fourier spectra, G(f), has constant magnitude in frequency domain.

$$F\{g(t-a)\} = \int_{-\infty}^{\infty} g(t-a) e^{-2\pi i x\xi}$$

That is, a time delay does not cause frequency content of G(f) to change at all. Since data points in case of an image, are discrete pixels, the discrete Fourier transform is applied rather than using continuous Fourier transform. To make the calculations faster, the fast Fourier transform is used.

C. Need for Log – Polar conversion

Although an image is a two dimensional flat representation of intensity values, laid out on x – y plane, a scaling or rotation alters the spatial resolution and pixel wise relative frequency content. Analysing this effect is beyond the scope of Cartesian coordinate plane. A much adaptable and easy to project coordinate system is provided by log – polar system. The mapping of Cartesian axes on logarithmic scale explains the scaling. The amount of scaling is given by radius of circle of polar plane. The conversion of Cartesian parameters into log – polar space parameters include the following relations,

$$r = \sqrt{x^2 + y^2}$$

where r is radius of circle circumscribing the rectangle bound by x and y axes.
The original image is in Cartesian plane. If the circle is inscribed inside the rectangle as the conversion boundary, some data points i.e. pixels lying outside may get ignored.Even if the conversion boundary circumscribes the rectangle, unwanted pixels may get covered and sampled. Since direct mapping of pixels from Cartesian to log polar space is not possible, average of central pixel and its neighbours is taken.The parameters of polar space, (ρ, θ), used to represent input image are related to parameters of polar space used to represent output image, by

$$(\rho, \theta) = (e^r, \theta)$$

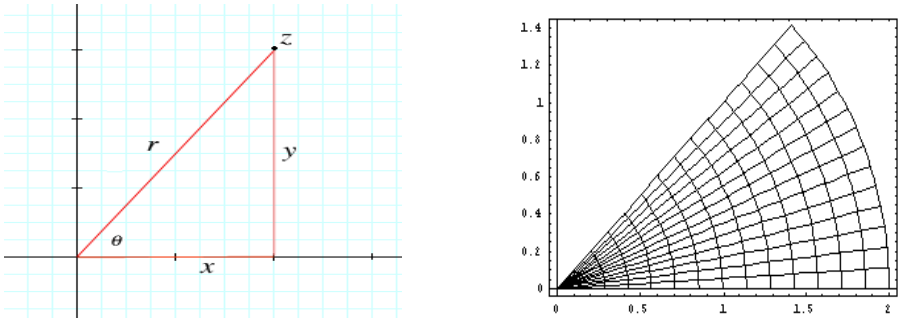

Fig 1: Log polar coordinate system

To map a random pixel (i, j) from input image, (x_i, y_j), onto (m, n) axes of output image, (r_m, θ_n), the following relation was used

$$x_i = \text{round}\ (\rho_m * \cos(\theta_n) + m_0)$$
$$y_j = \text{round}\ (\rho_m * \sin(\theta_n) + n_0)$$

where (m_0, n_0) is the central pixel.

D. Mellin transform

The Mellin transform [6,7] is used to create a transform space where the input image can be mapped onto output coordinate space which is rotation, scale as well as translation invariant. If some affine transformations are made to image in Cartesian plane, a DFT performed on same image transformed in log polar coordinate system shall recover all the changes. To speed up the calculations, we apply Fast Fourier transform instead of Discrete Fourier Transform.

The N periodic conventional Discrete Fourier Transform is given as

$$X_k = \sum_{n=0}^{N-1} x_n \cdot e^{-\frac{i2\pi kn}{N}}, \qquad \begin{matrix} n \in N \\ k = 0, \dots, N-1 \end{matrix}$$

But discrete Fourier transform decomposes the values into frequency components slowly. FFT on other hand, factorizes the N different combinations of transformations into sparse matrices. As a result, anyone can be easily accessed as a matrix component. It is also beneficial because sparse matrices are easily compressible due to lesser and only significant non zero elements. Hence, computational time is less. This algorithm can factorize the DFT matrix in either N^2or N log (N) operations. The fast Fourier transform, decimation in time, is given by the following mathematical expression

$$\sum_{n=0}^{N-1} a_n e^{-2\pi ink/N} = \sum_{n=0}^{\frac{N}{2}-1} a_{2n} e^{-2\pi i(2n)k/N} + \sum_{n=0}^{\frac{N}{2}-1} a_{2n+1} e^{-2\pi i(2n+1)k/N}$$

$$= \sum_{n=0}^{\frac{N}{2}-1} a_n^{even} e^{-\frac{2\pi ink}{N/2}} + e^{-2\pi ik/N} \sum_{n=0}^{\frac{N}{2}-1} a_n^{odd} e^{-\frac{2\pi ink}{N/2}}$$

In this study, the images were outsourced. The images are in binary format. Each one has a dimension of 120 by 120 pixels.

3. RESULTS

A. Similar Dermal Patterns

i. RADIAL LOOP – RADIAL LOOP

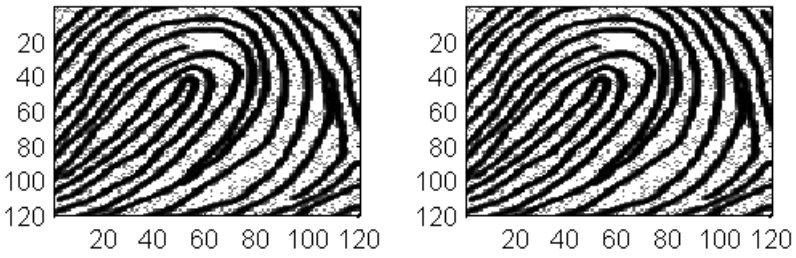

Fig 1 - Template and Test image – Radial Loop

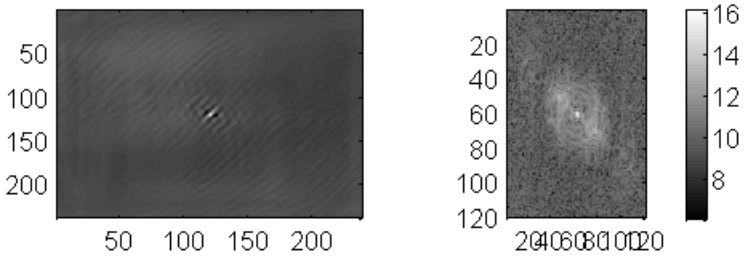

Fig 2 - High pass filtered spectrum of input image (using windowing technique)

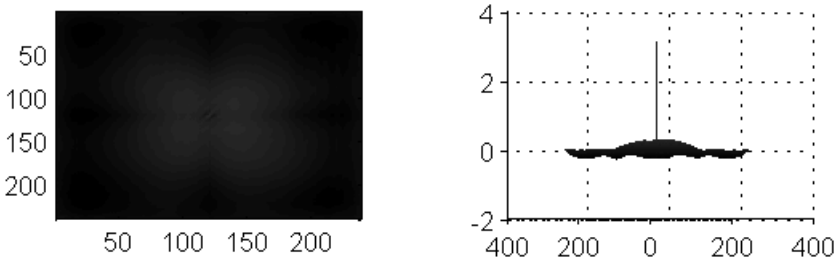

Fig 3 - Phase and Magnitude Correlation between test and template

ii. TENTED ARCH – TENTED ARCH

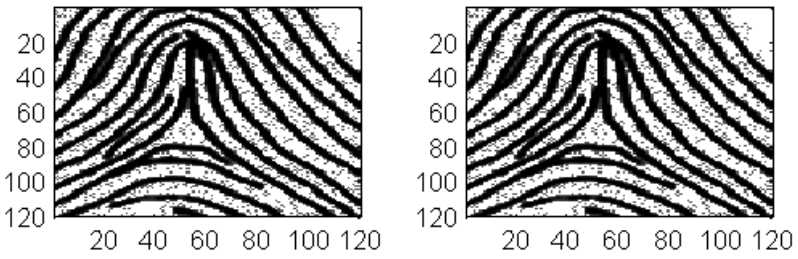

Fig 4 - Template and Test images – Tented arch

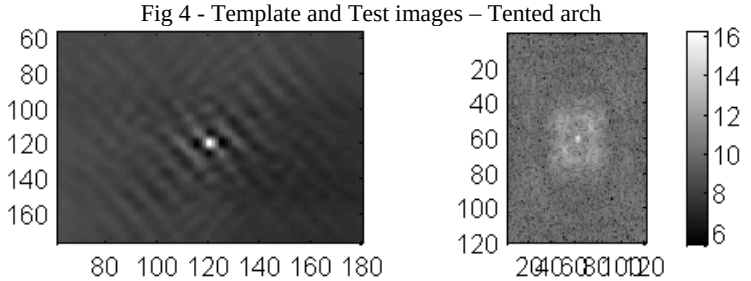

Fig 5 - High pass filtered spectrum of input image (using windowing technique)

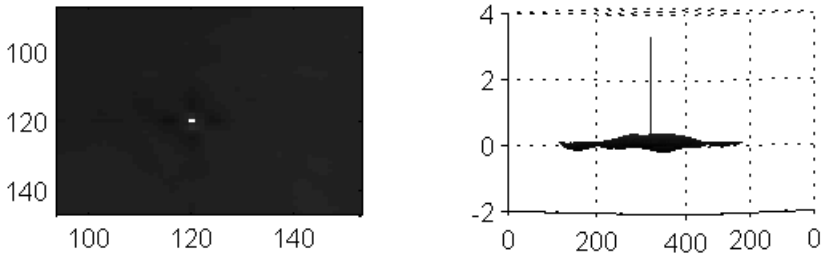

Fig 6 - Phase and Magnitude Correlation between test and template

iii. ULNAR LOOP – ULNAR LOOP

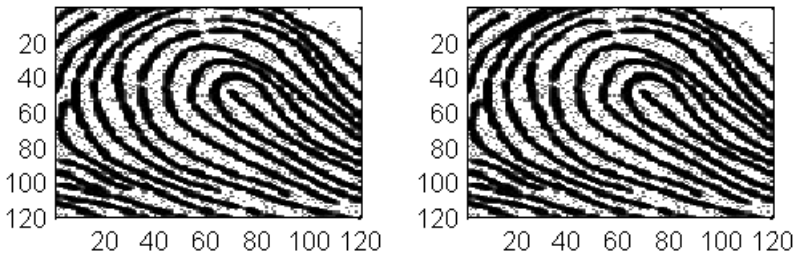

Fig 7 - Template and Test image – Ulnar Loop

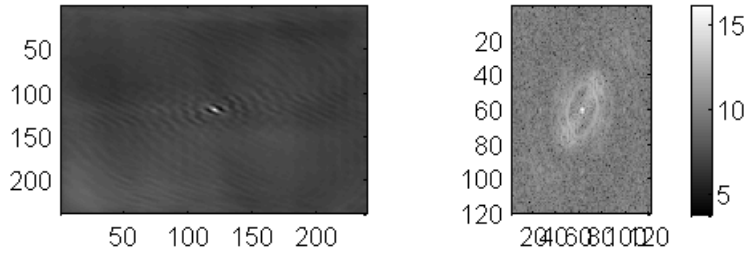

Fig 8 - High pass filtered spectrum of input image (using windowing technique)

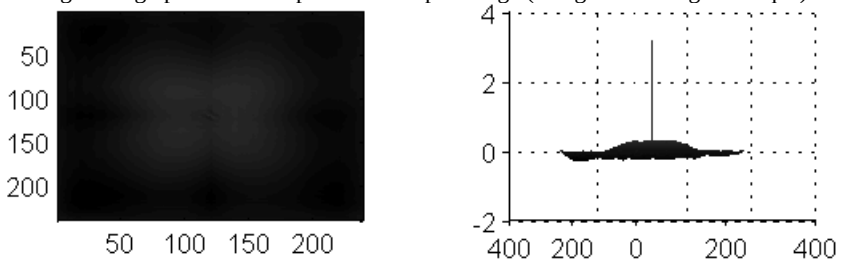

Fig 9 - Phase and Magnitude Correlation between test and template

iv. WHORL – WHORL

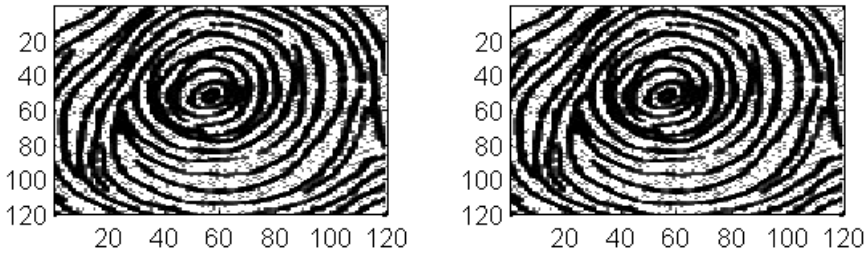

c

Fig 10 - Template and Test image – Whorl

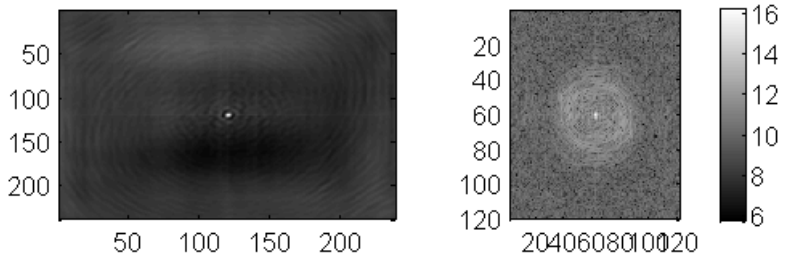

Fig 11 - High pass filtered spectrum of input image (using windowing technique)

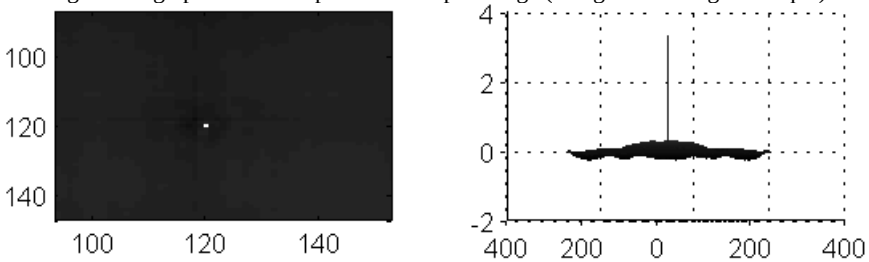

Fig 12 - Phase and Magnitude Correlation between test and template

B. Different Dermal Patterns

i. TENTED ARCH – VARIANT

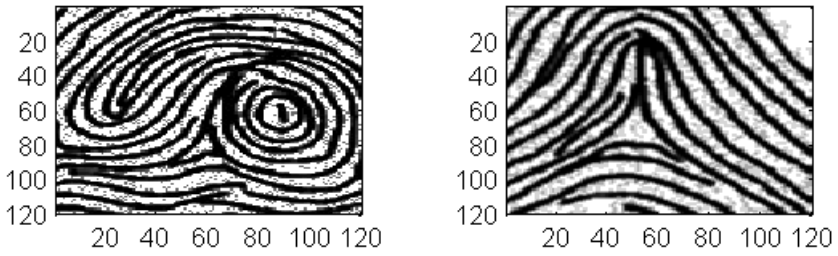

Fig 13 - Template and Test image – Variant and Tented Arch

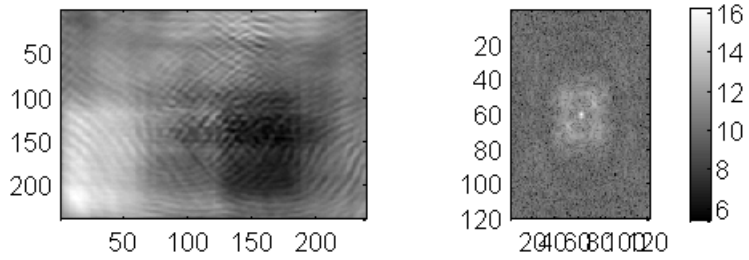

Fig14 - High pass filtered spectrum of input image (using windowing technique)

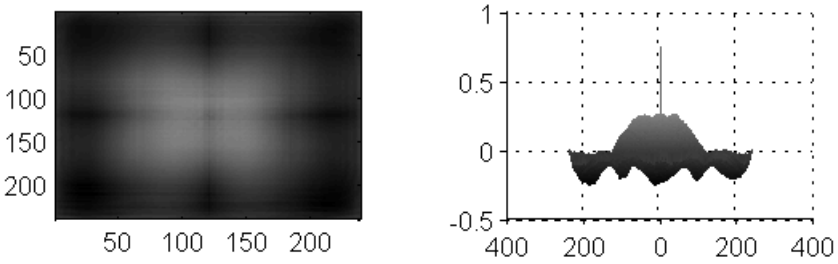

Fig 15 - Phase and Magnitude Correlation between test and template

ii. ULNAR LOOP – VARIANT

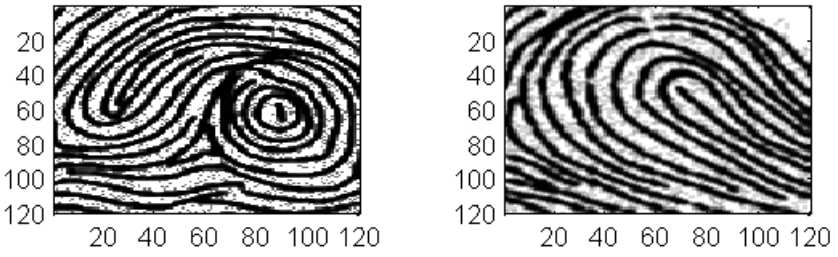

Fig 16 - Template and Test image – Variant and Ulnar loop

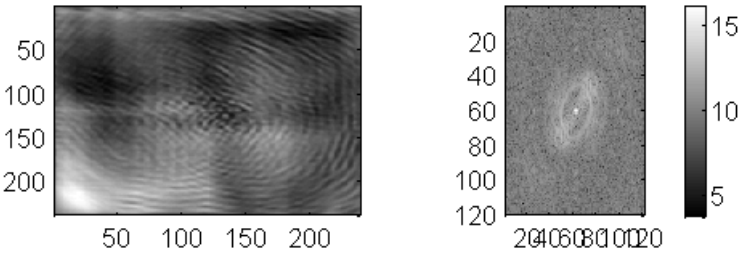

Fig 17 - High pass filtered spectrum of input image (using windowing technique)

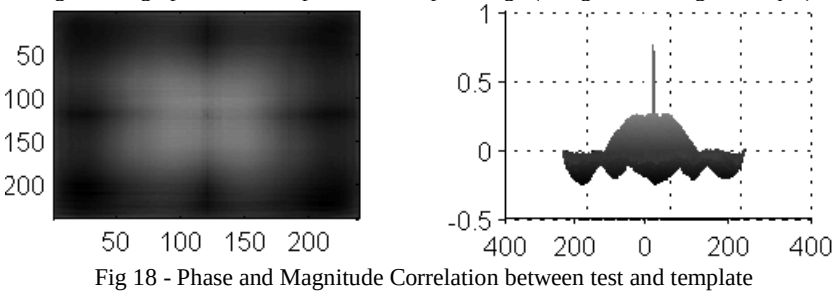

Fig 18 - Phase and Magnitude Correlation between test and template

iii. WHORL – ARCH

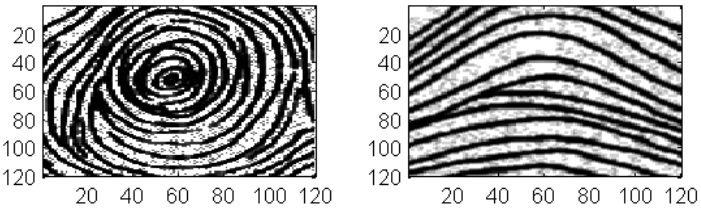

Fig 19 - Template and Test image – Whorl and Arch

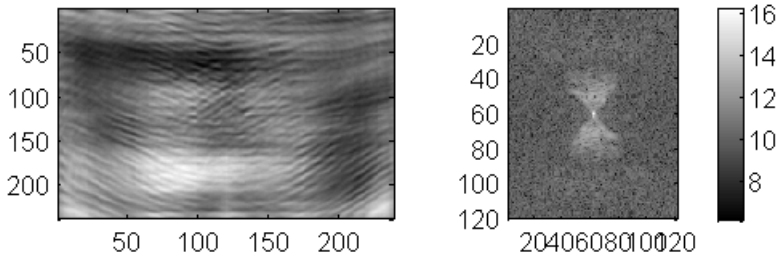

Fig 20 - High pass filtered spectrum of input image (using windowing technique)

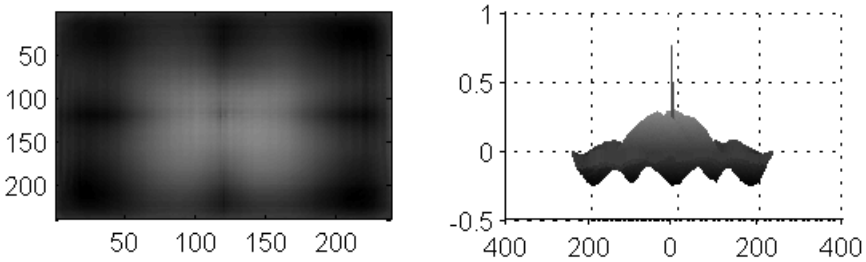

Fig 21 - Phase and Magnitude Correlation between test and template

iv. WHORL – RADIAL LOOP

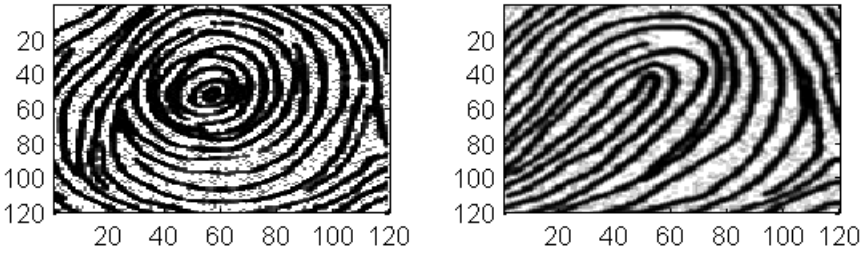

Fig 22 - Template and Test image – Whorl and Radial loop

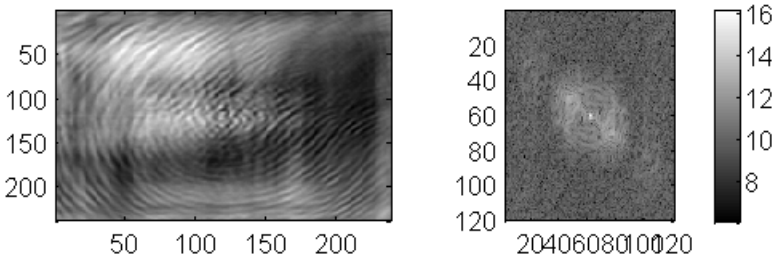

Fig 23 - High pass filtered spectrum of input image (using windowing technique)

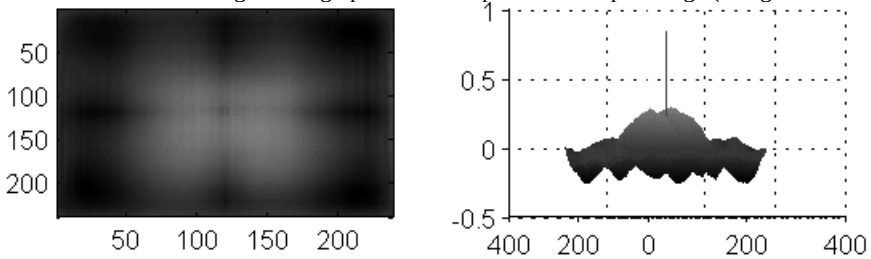

Fig 24 - Phase and Magnitude Correlation between test and template

v. WHORL – TENTED ARCH

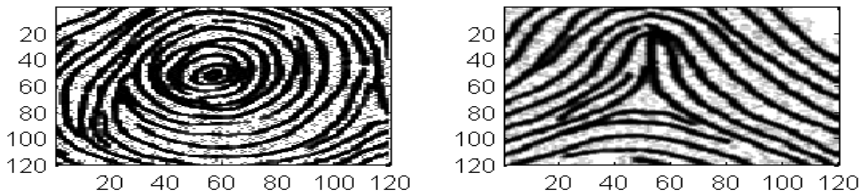

Fig 25 - Template and Test image – Whorl and Tented arch

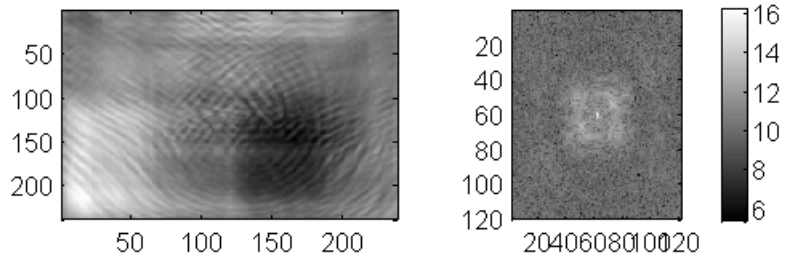

Fig 26 - High pass filtered spectrum of input image (using windowing technique)

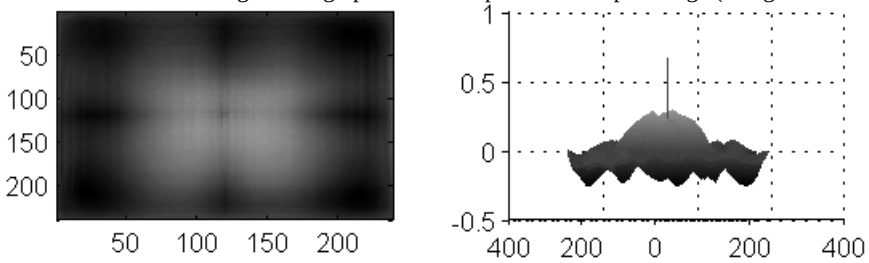

Fig 27 - Phase and Magnitude Correlation between test and template

vi. WHORL – ULNAR LOOP

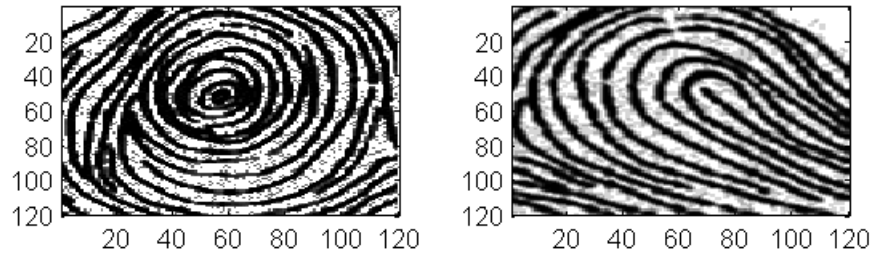

Fig 28 - Template and Test image – Whorl and Ulnar loop

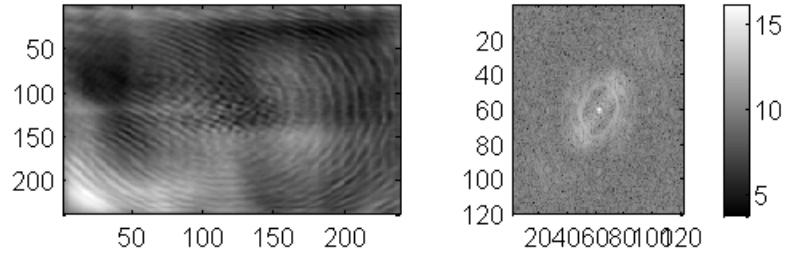

Fig 29 - High pass filtered spectrum of input image (using windowing technique)

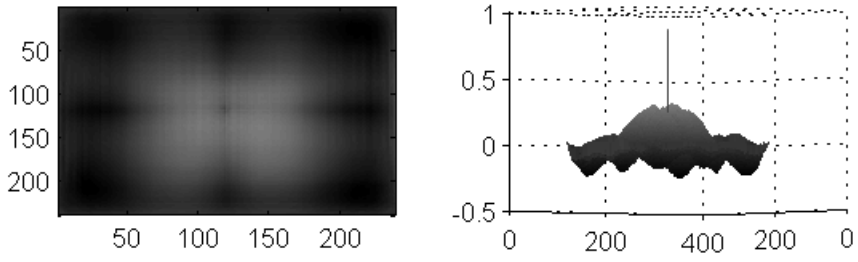

Fig 30 - Phase and Magnitude Correlation between test and template

vii. WHORL – VARIANT

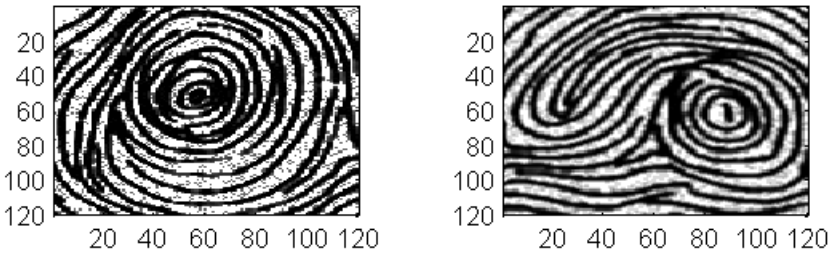

Fig 31 - Template and Test image – Whorl and Variant

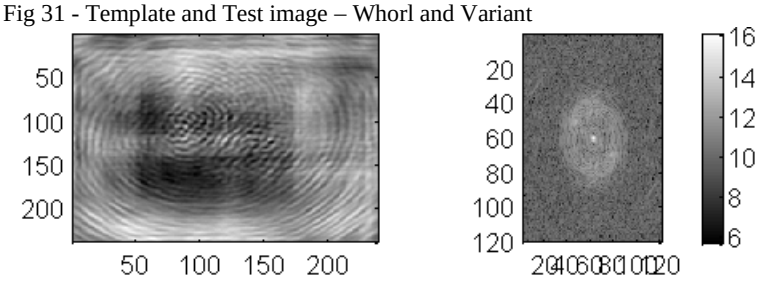

Fig 32 - High pass filtered spectrum of input image (using windowing technique)

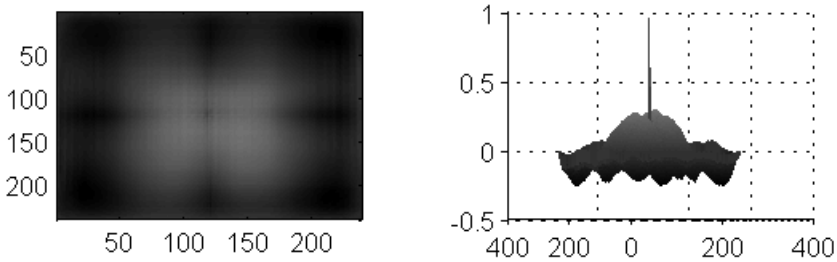

Fig 33 - Phase and Magnitude Correlation between test and template

viii. RADIAL LOOP – ULNAR LOOP

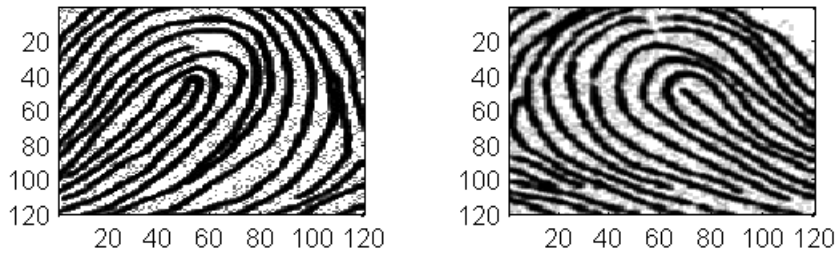

Fig 34 - Template and Test image – Radial loop and Ulnar loop

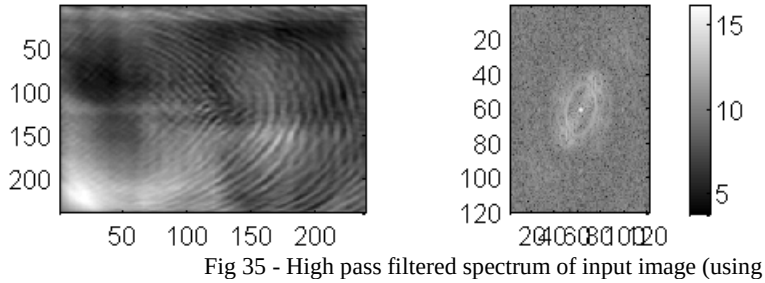

Fig 35 - High pass filtered spectrum of input image (using windowing technique)

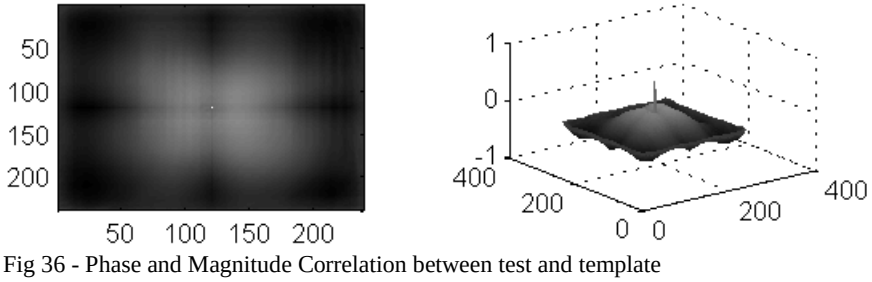

Fig 36 - Phase and Magnitude Correlation between test and template

ix. RADIAL LOOP – VARIANT

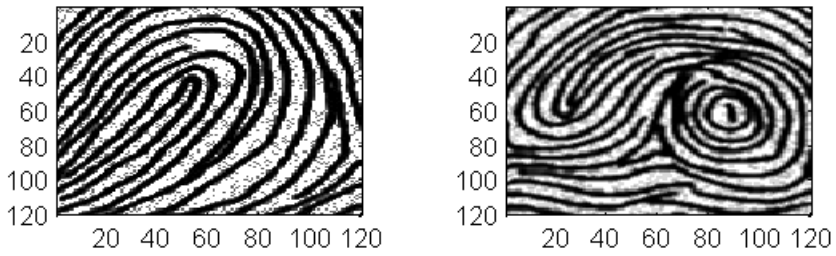

Fig 37 - Template and Test image – Radial loop and Variant

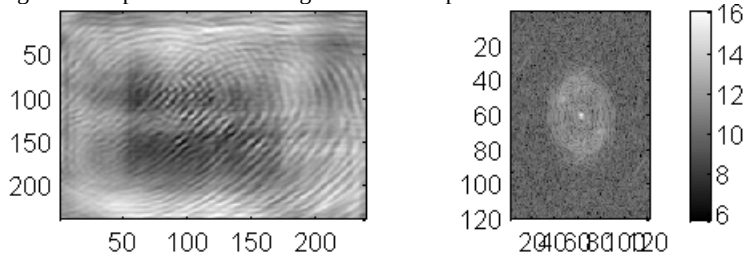

Fig 38 - High pass filtered spectrum of input image (using windowing technique)

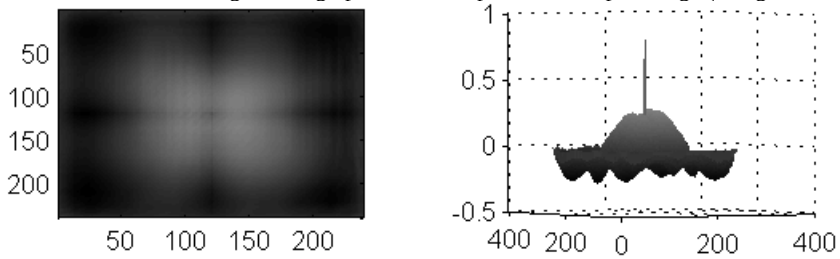

Fig 39 - Phase and Magnitude Correlation between test and template

x. RADIAL LOOP – TENTED ARCH

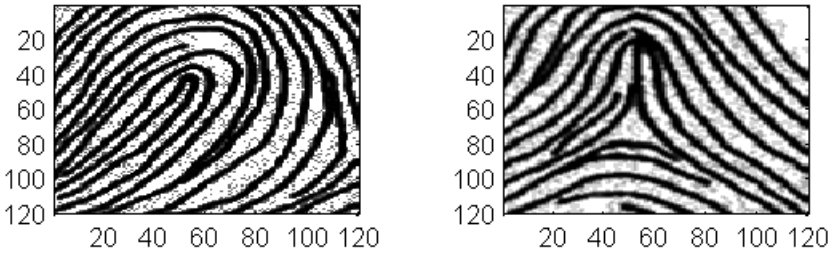

Fig 40 - Template and Test image – Radial loop and Tented arch

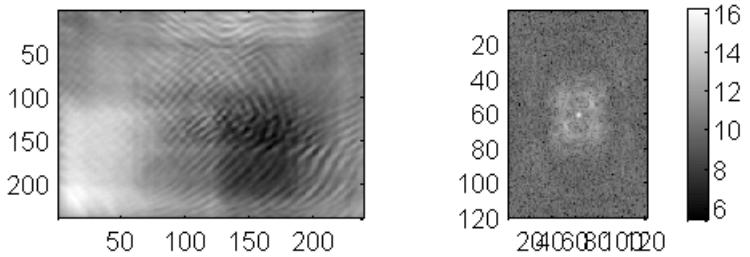

Fig 41 - High pass filtered spectrum of input image (using windowing technique)

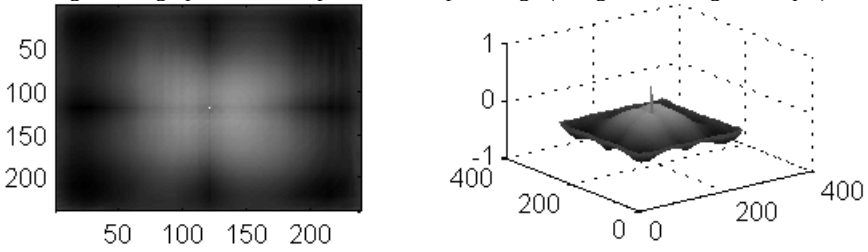

Fig 42 - Phase and Magnitude Correlation between test and template

xi. ULNAR LOOP – TENTED ARCH

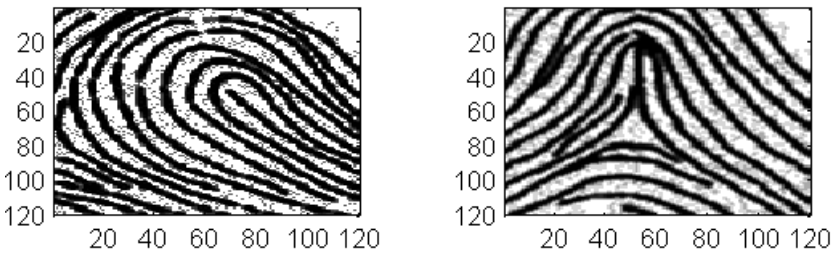

Fig 43 - Template and Test image – Ulnar loop and Tented arch

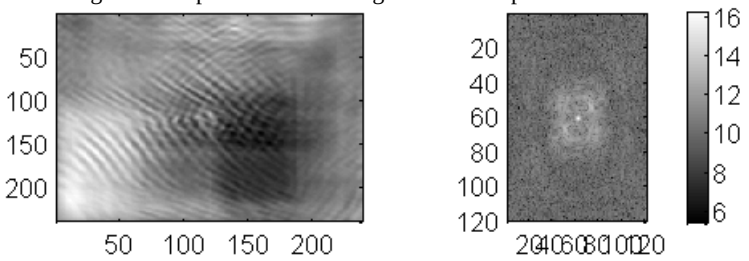

Fig 44 - High pass filtered spectrum of input image (using windowing technique)

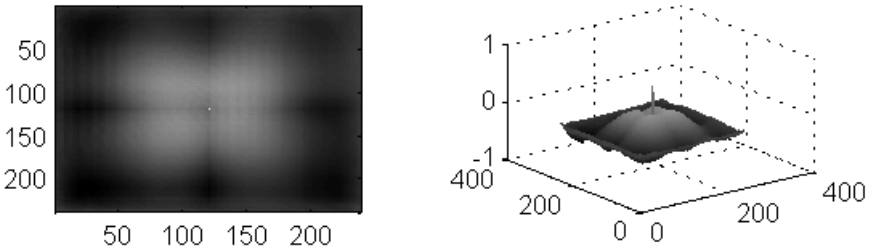

Fig 45 - Phase and Magnitude Correlation between test and template

C. Overall spectrum behaviour

Amongst all the patterns that were correlated amongst each other, it was found that when the test and template images were of same pattern, the amplitude spectrum of correlation matrix showed a singular maxima with a rough estimate on standard deviation found to be 3.3, which is quite high. This signifies that that the maxima has been a true positive. The peak is attained at centre of x-y plane since the peak has been zero shifted after the correlation matrix was FFT filtered. Those where two different patterns are being matched display multiple peaks. This signifies that due to similarity of curvature amongst dermal patterns at some places give rise to such peaks. It is important know that these peaks have magnitude almost half of the maxima that was obtained in previous case. Same behaviour has been observed in case of phase correlation plots.

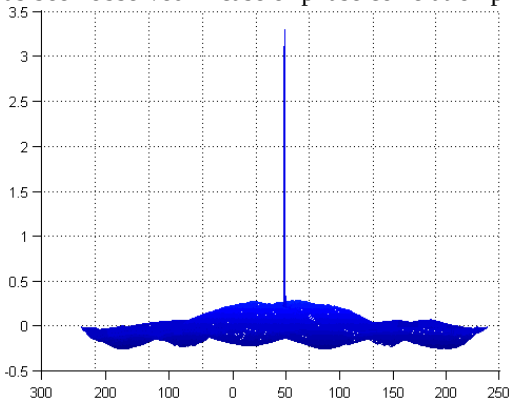

Fig 46 - Amplitude spectrum of correlation matrix of matched patterns

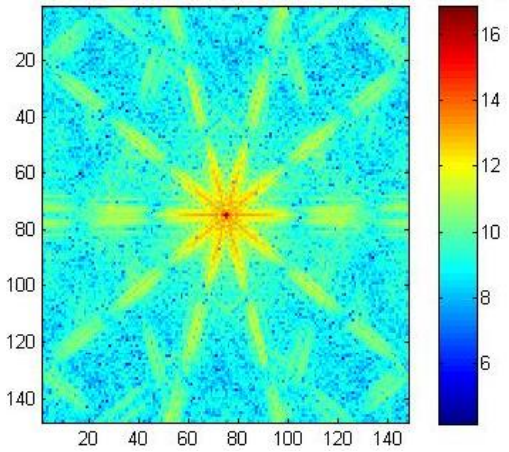

Fig 47 - High pass filtered magnitude spectrum (post windowing)

Each pattern is cross-correlated with every other pattern. For the algorithm to function properly, the correlation score between similar patterns must be higher than between different patterns. Apart from tented arch, all other patterns have shown highest correlation score when matched to themselves. To validate the reliability of the algorithm, comparisons have been done in normalized scale, i.e. all comparison scores within one pattern category come under same scale. The graphic is given in chart 1.

	Whorl	Arch	Tented arch	Radial loop	Ulnar loop	Variant
Whorl	0.634	0.458	0.395	0.509	0.448	0.483
Arch		2.044	0.342	0.95	1.716	-4.061
Tented arch			0.554	0.85	1.688	4.066
Radial loop				1.148	0.929	0.952
Ulnar loop					1.899	-4.022
Variant						-3.87

Chart 1 – Score display of all patterns correlated to every other pattern

The following charts from 2 to 7 display scores of six categories of patterns individually correlated with all patterns, including itself.

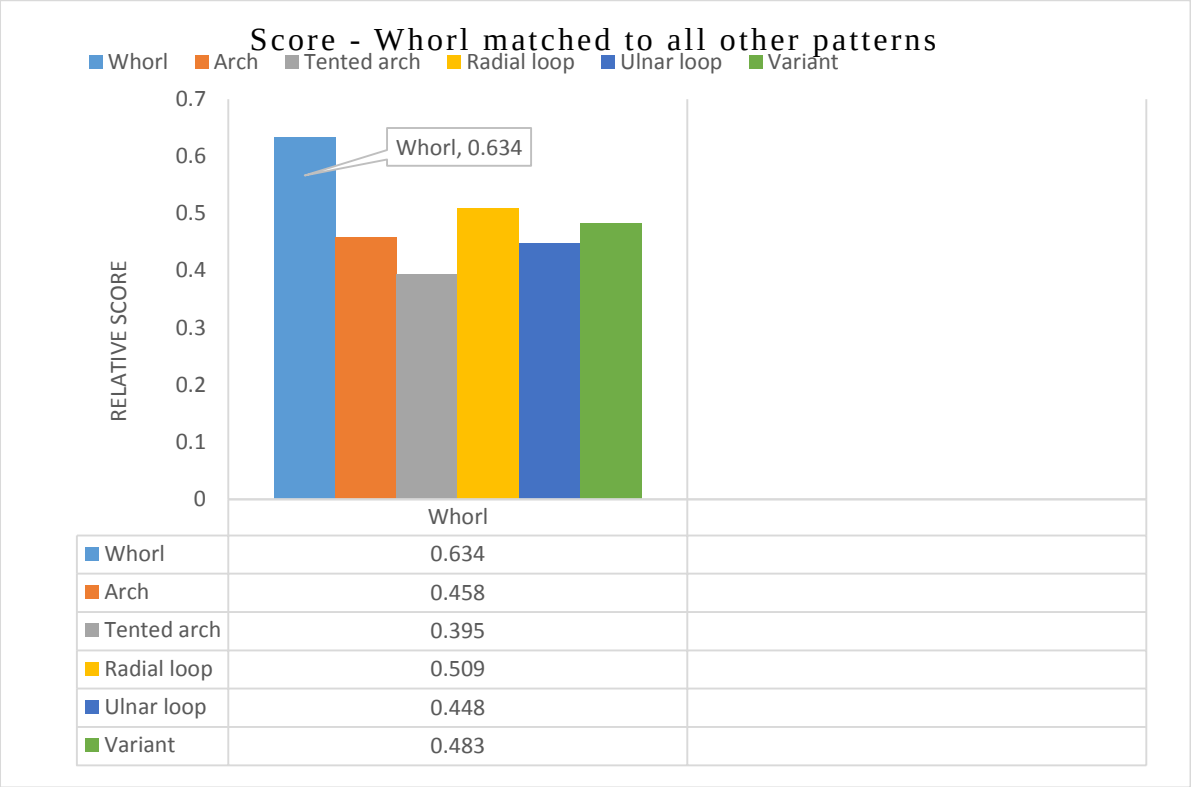

	Whorl
Whorl	0.634
Arch	0.458
Tented arch	0.395
Radial loop	0.509
Ulnar loop	0.448
Variant	0.483

Chart 2 – Score display of Whorl correlated to all patterns

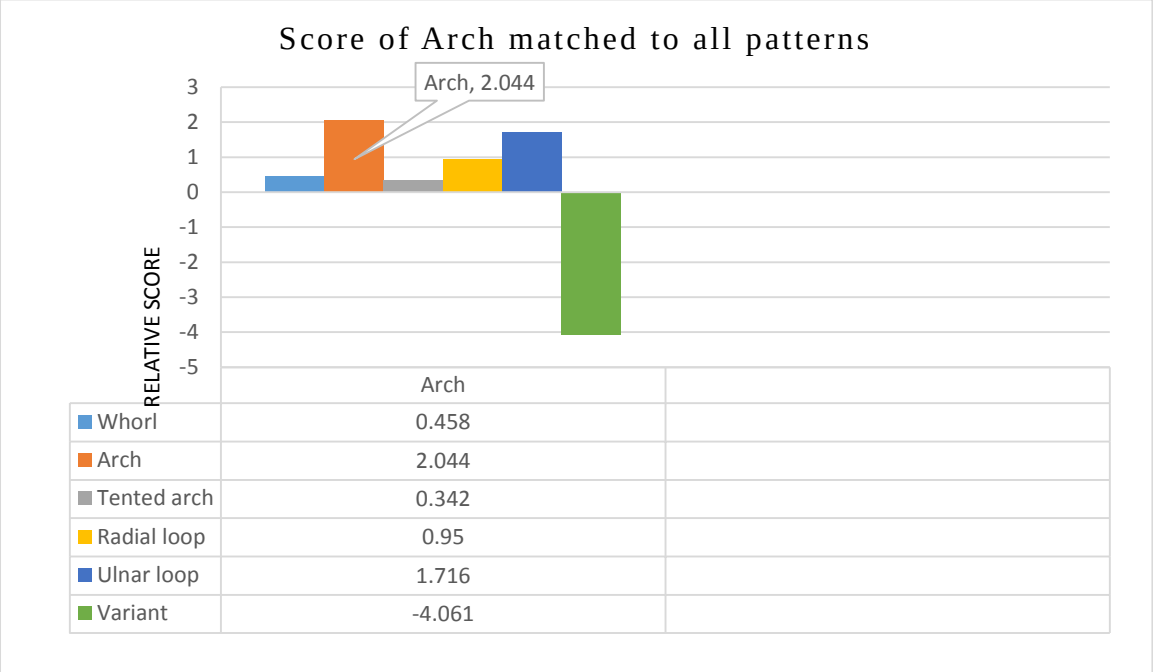

	Arch
Whorl	0.458
Arch	2.044
Tented arch	0.342
Radial loop	0.95
Ulnar loop	1.716
Variant	-4.061

Chart 3 – Score display of Arch correlated to all patterns

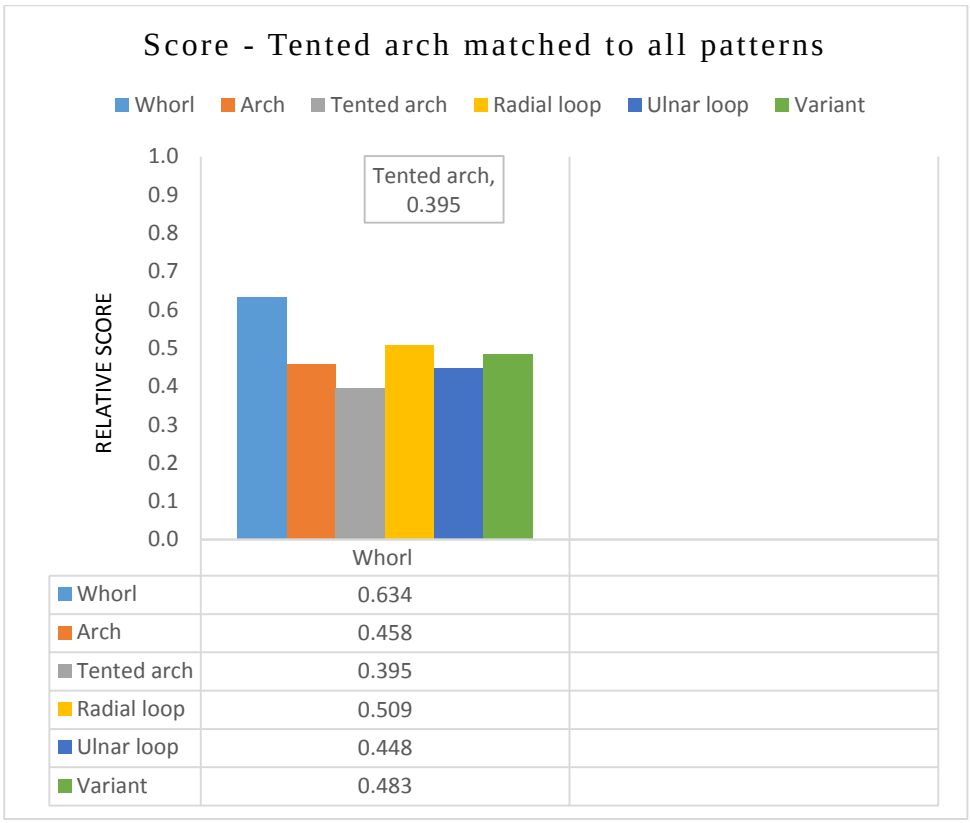

Chart 4 – Score display of Tented arch to all patterns

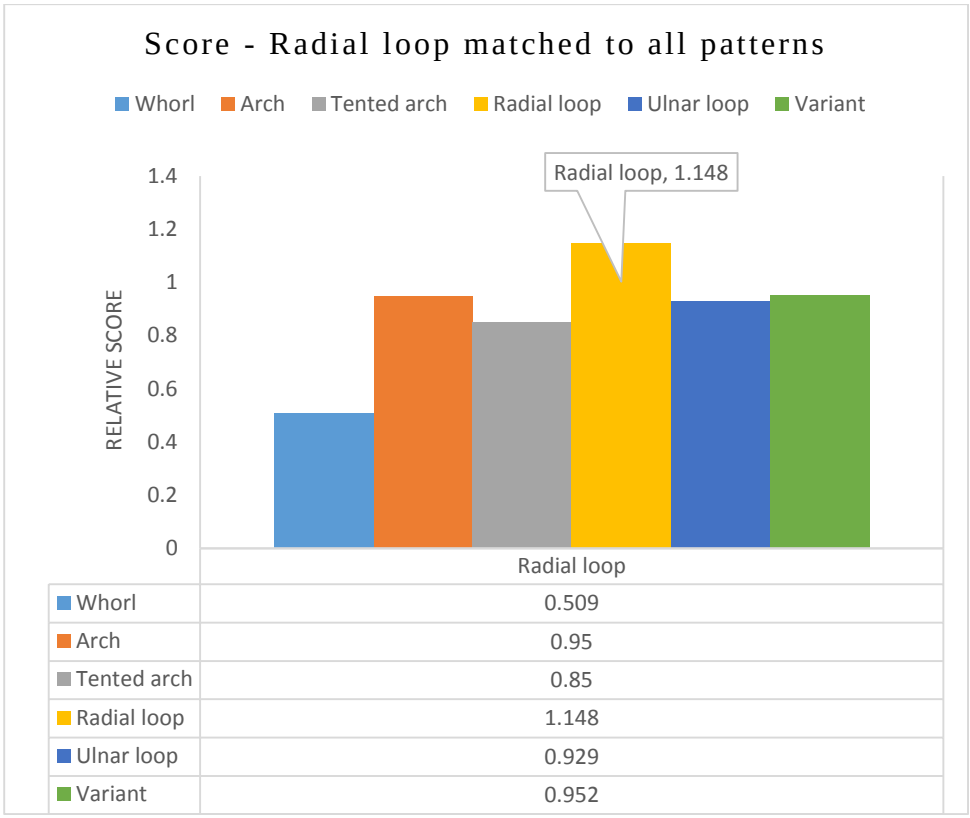

Chart 5 – Score display of Radial loop correlated to all patterns

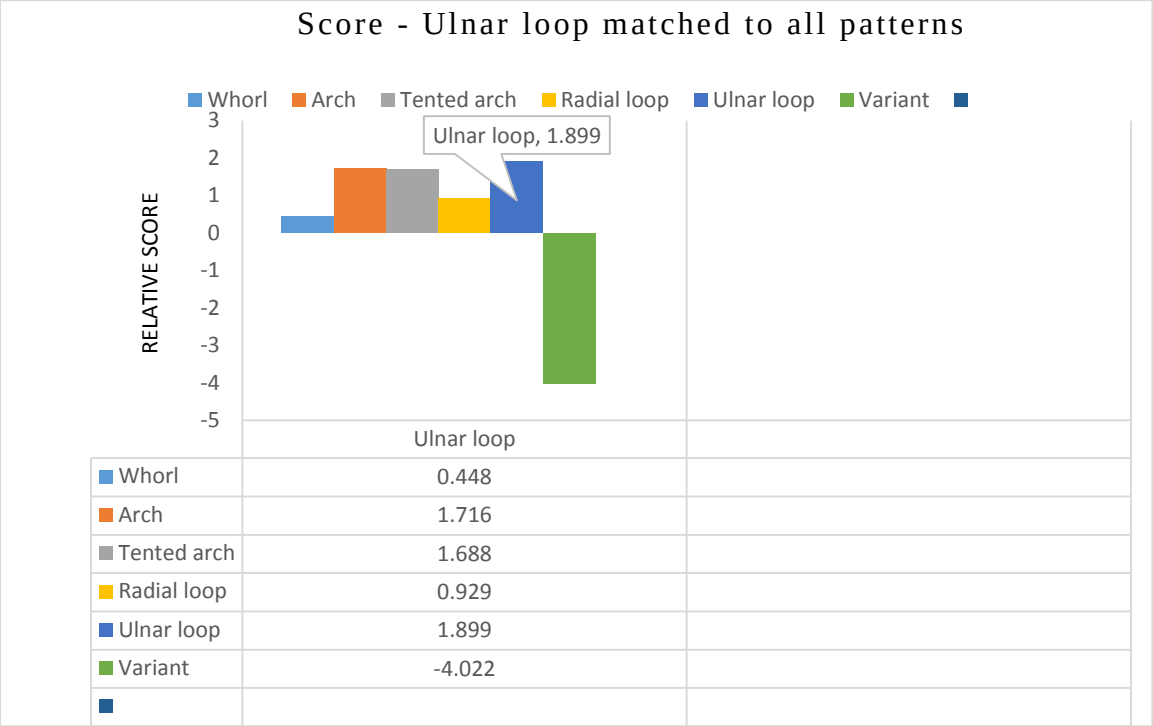

Chart 6 – Score display of Ulnar loop correlated to all patterns

Expected result

	Whorl	**Arch**	**Tented arch**	**Radial loop**	**Ulnar loop**	**Variant**
Whorl	High					
Arch		High				
Tented arch			High			
Radial loop				High		
Ulnar loop					High	
Variant						High

Obtained result

	Whorl	**Arch**	**Tented arch**	**Radial loop**	**Ulnar loop**	**Variant**
Whorl	High					
Arch		High				
Tented arch						High
Radial loop				High		
Ulnar loop					High	
Variant						High

4. CONCLUSION

The work concludes that the Fourier Mellin transform is an effective method for registering affine transforms in original images. The algorithm was tested for six dermatoglyphical patterns, namely : Arch, Tented arch, Whorl, Radial loop, Ulnar loop and Variant. All similar patterns have displayed highest correlation when the algorithm was applied between the original image and the transformed image. This infers that when all the six patterns

were auto correlated with their affine transformed version, five out of six patterns showed complete match. Also, when two different patterns were correlated, the phase as well as magnitude plot shows presence of side harmonics along with a not so sharp zero centred maxima. This proves that the algorithm fails to gain a single sharp global maxima in cases of different patterns. One can conclude that all the patterns when correlated with affine transformed versions of others patterns, they showed mismatch of patterns.

REFERENCES

[1]. Mandeep Singh, Oindri Majumdar, "Dermatoglyphics : Blueprints of Human Cognition on Fingerprints", International Journal of Computer Science and Communication, Vol. 6, No. 2, Sept 2015

[2]. Mandeep Singh, Mahak Narang, "Cognitive Enhancement Techniques", International Journal of IT and Knowledge Management, Vol. 7, Issue 2, 2015

[3]. Mandeep Singh, Oindri Majumdar, "Image processing techniques in Dermatoglyphic fingerprint analysis : A review", International Journal of Computer Science and Communication, Vol. 6, No. 2, Sept 2015

[4]. Knapp, Charles H., and G. Clifford Carter, "The generalized correlation method for estimation of time delay" Acoustics, Speech and Signal Processing, IEEE Transactions on 24.4: 320-327, 1976

[5]. Stefano, Luigi Di, Stefano Mattoccia, and Martino Mola, "An efficient algorithm for exhaustive template matching based on normalized cross correlation.", Proceedings 12th International Conference onImage Analysis and Processing, IEEE, 2003

[6]. R.M. Mandi, S.S. Lokhande, "Rotation Invariant Fingerprint Identification System", International Journal of Electronics Communication and Computer Technology (IJECCT) Volume 2 Issue 4, July 2012

[7]. Lin, Wu, Bloom, Cox, Miller, Lui , "Rotation, Scale and Translation Resilient Watermarking for Images", IEEE transactions on Image Processing, Vol. 10, No. 5, pp. 767-782, May 2001